

Comprehensive investigation of the non-covalent binding of MRI contrast agents with human serum albumin

Virginie Henrotte · Luce Vander Elst ·
Sophie Laurent · Robert N. Muller

Received: 14 February 2007 / Accepted: 2 May 2007 / Published online: 9 June 2007
© SBIC 2007

Abstract Three techniques, electrospray mass spectrometry, ultrafiltration, and proton relaxometry, are compared in the context of the quantitative analysis of non-covalent binding between human serum albumin (HSA) and MRI contrast agents. The study of the affinity by proton relaxometry reveals the association constant and the number of interaction sites assuming that all sites are identical and independent. Ultrafiltration was adapted for the study of paramagnetic complexes. This technique confirmed the results obtained by relaxometry. Electrospray mass spectrometry, an original method able to study non-covalent binding because of its soft ionization process that allows for the survival of weak binding, provides qualitative and quantitative results. Electrospray mass spectrometry confirmed the affinity measured by proton relaxometry and ultrafiltration. This technique requires very small amounts of products and directly gives the stoichiometry of the association, information not easily obtained by classic techniques. Nevertheless, proton relaxometry remains a useful and mandatory technique for determining the enhancement of the relaxation subsequent to the binding although it demands large amounts of compounds. It is to be pointed out that even if the three techniques lead to a similar ranking of the affinity of the contrast agents for HSA, the absolute values of the association constants disagree as a result of the difference in the experimental conditions (presence of salt, native protein or desalted one,

approximations in the fitting of the data, liquid or gas phases).

Keywords Contrast agent · Human serum albumin · Binding · Mass spectrometry · Relaxivity

Introduction

Magnetic resonance imaging (MRI) is a powerful and non-invasive diagnostic technique useful in providing anatomical and functional images of the human body. At present, a large number of MRI scans are performed employing a paramagnetic compound able to enhance the image contrast by increasing the nuclear relaxation rate of water protons in the surrounding tissues. The most frequently used contrast agents are gadolinium polyaminocarboxylic complexes, because of the favorable physicochemical properties of this lanthanide: seven unpaired electrons, nine coordination sites, and favorable electronic relaxation time. The complexation of this rare-earth ion with an organic ligand like a polycarboxylic acid is necessary to minimize its toxicity but reduces to some extent its efficacy as the active core of the contrast agent [1, 2]. The additional presence of a lipophilic component on the gadolinium(III) chelate allows for the formation of non-covalent interactions between the gadolinium(III) complex and an endogenous blood macromolecule, human serum albumin (HSA) [3–7].

Thanks to its high concentration in blood, HSA is of interest in imaging because its binding to contrast agents significantly increases their vascular residence time and contrasting ability making them favorable for angiographic applications of MRI. Among such contrast agent derivatives, *S*-4-(4-ethoxybenzyl)-3,6,9-tris(carboxymethyl)-

V. Henrotte · L. Vander Elst · S. Laurent · R. N. Muller (✉)
Department of General, Organic and Biomedical Chemistry,
NMR and Molecular Imaging Laboratory,
University of Mons-Hainaut,
Avenue du Champ de Mars,
24 B-7000 Mons, Belgium
e-mail: robert.muller@umh.ac.be

3,6,9-triazaundecanedioic acid, gadolinium complex (Gd-EOB-DTPA; Eovist[®]) and (9*R,S*)-2,5,8-tris(carboxymethyl)-12-phenyl-11-oxa-2,5,8-triazadodecane-1,9-dicarboxylic acid, gadolinium complex (Gd-BOPTA; MultiHance[®]) have shown an extended blood half-life owing to their moderate non-covalent binding to HSA [8–11]. Another blood pool agent, the gadolinium(III) complex of 4-pentylbicyclo[2.2.2]octane-1-carboxyldi-*L*-aspartyllysine DTPA, known as MP-2269 [12–14], provides excellent vascular enhancement because of a reversible binding to human serum albumin owing to its non-aromatic side chain. MS-325 [15, 16], a Gd-DTPA derivative, {4-(*R*)-[(4,4-diphenylcyclohexyl)phosphonooxymethyl]-3,6,9-triaza-3,6,9-tris(methoxycarbonyl)undecanedioato}gadolinium, possesses a lipophilic diphenylcyclohexyl group attached to one of the ethylene bridges of the backbone by means of a phosphodiester linkage. The simultaneous presence of this lipophilic substitute and of the negatively charged phosphodiester is responsible for the non-covalent binding interaction with HSA and induces also an excellent vascular enhancement [15, 16, 25]. More recently, a contrast agent named B-22956/1 [17, 18], whose molecular structure features a polyaminocarboxylate gadolinium(III) complex linked to a deoxycholic acid moiety by means of a flexible spacer, was reported to have a high affinity for serum albumin (Fig. 1).

In the present work, we investigate the affinity of these contrast agents for HSA by three different techniques: proton relaxometry, ultrafiltration, and electrospray mass spectrometry. Each of these techniques is based on a different background. Proton relaxometry allows estimation of the binding of a contrast agent to a macromolecule through the water proton relaxation rate. In fact, the decrease of mobility of the contrast agent due to the interaction with a large molecule leads to an increase of the proton relaxation rate and consequently improves its efficiency. The relaxation enhancement reflects the affinity of the contrast agent for HSA. In this work, the affinity by proton relaxometry is studied for solutions containing a fixed concentration of HSA and increasing concentrations of the contrast agent. The increase in efficiency of the contrast agent in the presence of the protein and the non-linear evolution of the relaxation rate indicate that the ligand has an affinity for the target.

Ultrafiltration is a more usual technique, where information on the affinity is evaluated by measuring the free ligand concentration [19, 20].

Electrospray ionization mass spectrometry (ESI-MS) is emerging as a new method to study biomolecular non-covalent interactions [21, 22]. The ability of ESI-MS to study specific non-covalent complexes is inherent to its soft ionization, which does not induce any unwanted molecular fragmentation, thus allowing weak non-covalent interactions to survive the electrospray process.

Materials and methods

Chemicals

Non-defatted HSA A-1653 was purchased from Sigma (Bornem, Belgium). For electrospray mass spectrometry, HSA was desalted by five dilution–concentration steps using Microcon YM-10 from Millipore (Brussels, Belgium). The protein concentration was measured spectrophotometrically (280 nm) (8452A diode-array spectrophotometer, Hewlett-Packard, Brussels, Belgium).

Gd-DTPA (Magnevist[®]), Gd-EOB-DTPA (Eovist[®]), and MS-325 (Vasovist[®]) were provided by Schering (Berlin, Germany). Gd-BOPTA (MultiHance[®]) and B-22956/1 were provided by Bracco (Milan, Italy). MP-2269 was given by Mallinckrodt (St. Louis, USA).

Ultrafiltration method

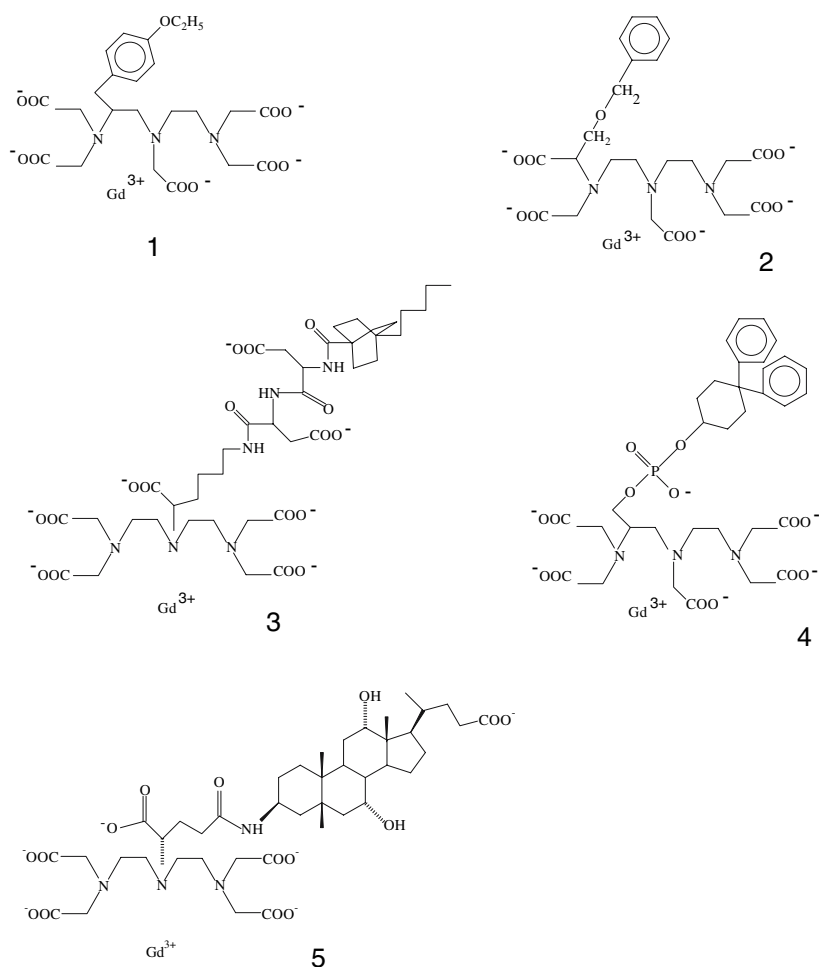
During the ultrafiltration measurements in HSA A-1653, the unbound ligand fractions were separated using the Ultrafree-4 centrifugal filter and Biomax-10K tube (Millipore) by centrifugation (1,547g, 3 min). All solutions were prepared in phosphate buffer (Na₂HPO₄ 10 mM, NaCl 150 mM, pH 7.4). The free ligand concentration was obtained by proton relaxometry (three to five *T*₁ measurements). The bound ligand concentration was calculated by subtracting the free ligand concentration from the initial concentration measured by relaxometry. The relative error on the *T*₁ measurements was 3%.

Proton relaxivity method

The proton paramagnetic relaxation rate data (*R*_{1,obs}^P) were obtained at fixed field strength (0.47 T) and temperature (310 K) using a Minispec pc-20 (Bruker, Karlsruhe, Germany). The proton data obtained in HSA A-1653 solution were fitted using Eq. 1:

$$R_{1,obs}^P = 1000 \left[r_1^f L_0 + (r_1^c - r_1^f) \left\{ \frac{NP_0 + L_0 + K^{-1} - \sqrt{(NP_0 + L_0 + K^{-1})^2 - 4L_0P_0}}{2} \right\} \right], \quad (1)$$

Fig. 1 Structures of Gd-EOB-DTPA (Eovist[®]; 1), Gd-BOPTA (MultiHance[®]; 2), MP-2269 (3), MS-325 (Vasovist[®]; 4), and B-22956/1 (5). For an explanation of the naming of the contrast agents, see the text



where K is the association constant, P_0 is the protein concentration, L_0 is the concentration of the paramagnetic complex, N is the number of independent and identical interaction sites, and r_1^c and r_1^f are the relaxivities of the HSA–contrast agent complex and the free contrast agent, respectively (per second per millimole liter).

Electrospray mass spectrometry method

Electrospray mass spectra were obtained using a Q-tof 2 (Micromass, Manchester, UK) at the Mass Spectrometry Center of the University of Mons-Hainaut. The nanospray source was operated in the positive ion mode at a capillary voltage of 1.4 kV. Samples, dissolved in ammonium acetate (100 mM), were injected with needles at a flow rate of a few nanoliters per minute. Each spectrum is the sum of approximately 400 scans. The raw spectra were then baseline-corrected before deconvolution, with the program MaxEnt1[™]. The concentration of albumin samples injected in the mass spectrometer was 5 μ M. All spectra were recorded at a cone voltage of 180 V and a source temperature of 353 K. The concentration of HSA was fixed at

5 μ M in ammonium acetate and the concentration of contrast agent ranged from 5 to 50 μ M.

Results and discussion

The ultrafiltration method

The protein–complex binding of three contrast agents, Gd-EOB-DTPA, Gd-BOPTA (Fig. 2), and MP-2269 (Fig. 3), was determined by ultrafiltration. The total concentration of contrast agent ranged from 0.1 to 2 mM for Gd-EOB-DTPA and Gd-BOPTA or 4 mM for MP-2269, while the protein concentration was fixed at 4%. The data are presented as concentrations of bound contrast agent divided by the fixed protein concentration versus the unbound ligand concentrations.

The binding constants were evaluated from a model assuming several sites of interaction (i sites) (Eq. 2):

$$\frac{PL}{P_0} = \sum_i \frac{n_i K_i L}{1 + K_i L} \quad (2)$$

Fig. 2 Ultrafiltration results: concentration of bound Gd-EOB-DTPA (a) and Gd-BOPTA (b) divided by P_0 versus their free concentrations

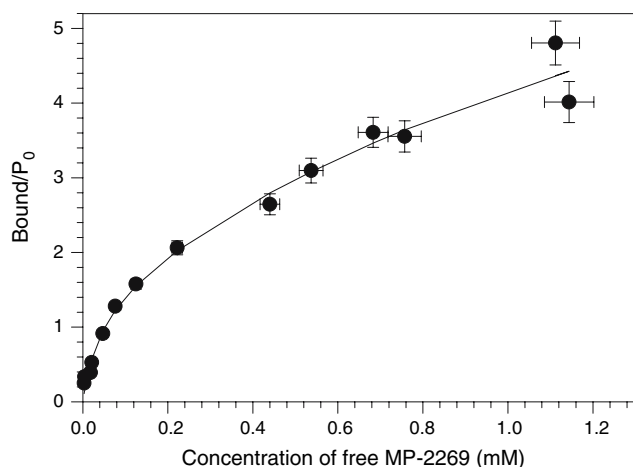
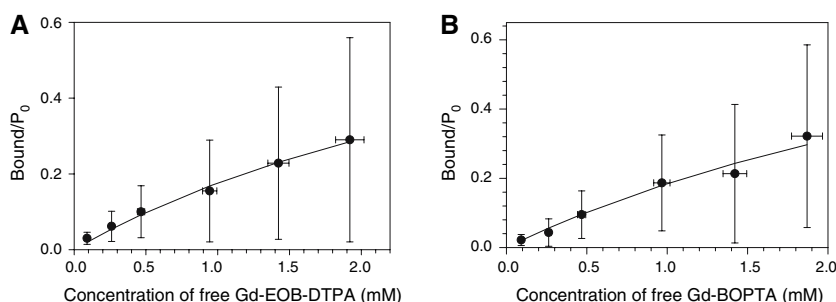


Fig. 3 Ultrafiltration results: concentration of bound MP-2269 divided by P_0 versus its free concentration

where P_0 is the protein concentration, L is the concentration of free contrast agent, PL is the concentration of the complex, K_i are the association constants, and n_i are the number of sites of interaction. Table 1 presents the results obtained from the fitting of the experimental data.

According to these experiments, Gd-EOB-DTPA and Gd-BOPTA have one site of interaction and quite a similar affinity for HSA. For MP-2269 two types of sites were found, one of which was characterized by a larger association constant. The errors on the fitting of MP-2269 are larger owing to the presence of different sites resulting in a larger number of parameters. The contrast agent Gd-DTPA has no lipophilic component allowing for the formation of non-covalent interactions. Indeed, after filtration, the free ligand concentrations are equivalent to the initial concentrations of Gd-DTPA. These results confirm the known absence of affinity.

Table 1 also shows the ultrafiltration data reported in the literature for MS-325 and B-22956/1 [16, 23, 24]. MP-2269 and MS-325 have an affinity constant on the order of 10^4 M^{-1} for the strongest site, whereas B-22956/1 has an association constant 10 times larger.

Proton relaxivity method

The proton paramagnetic relaxation rate was measured at 20 MHz on solutions containing 4% HSA ($P_0 = 0.6 \text{ mM}$) and various concentrations of contrast agent ($L_0 = 0\text{--}2 \text{ mM}$) (Fig. 4). As expected, the relaxation rates (R_1^p) of each paramagnetic complex in protein-free aqueous solution increase linearly with concentration (dashed and dotted lines). The slope of each line gives the relaxivity of the free complex. (Fig. 4) In HSA solution, the relaxation rates are significantly enhanced compared with those in pure water. For example, the paramagnetic relaxation rate of a solution containing 1 mM MP-2269 and 4% HSA is 5 times larger than that in pure water. Moreover, the non-linear increase of the proton paramagnetic relaxation rate in HSA solution agrees with a strong binding. The fitting of the data according to Eq. 1 yields an estimation of a global

Table 1 Results of the fitting of the ultrafiltration data shown in Figs. 2 and 3

Gd-EOB-DTPA	$n_1 = 0.87 \pm 0.23$ $K_1 = 255 \pm 90 \text{ M}^{-1}$
Gd-BOPTA	$n_1 = 1 \pm 0.58$ $K_1 = 226 \pm 170 \text{ M}^{-1}$
MP-2269	$n_1 = 1.4 \pm 0.5$ $K_1 = (24.7 \pm 13.7) \times 10^3 \text{ M}^{-1}$ $n_2 = 8.7 \pm 4.9$ $K_2 = 478 \pm 486 \text{ M}^{-1}$
MS-325 ^a	$n_{1,2,3,4} = 1$ $K_1 = (11.0 \pm 2.7) \times 10^3 \text{ M}^{-1}$ $K_2 = 840 \pm 160 \text{ M}^{-1}$ $K_3 = 260 \pm 140 \text{ M}^{-1}$ $K_4 = 430 \pm 240 \text{ M}^{-1}$
B-22956/1 ^b	$n_1 = 1$ $K_1 = 26.0 \times 10^4 \text{ M}^{-1}$

For an explanation of the naming of the contrast agents, see “Introduction.” The MS-325 and B-22956/1 data reported in the literature are shown for comparison

^a From [16]

^b From [23, 24]

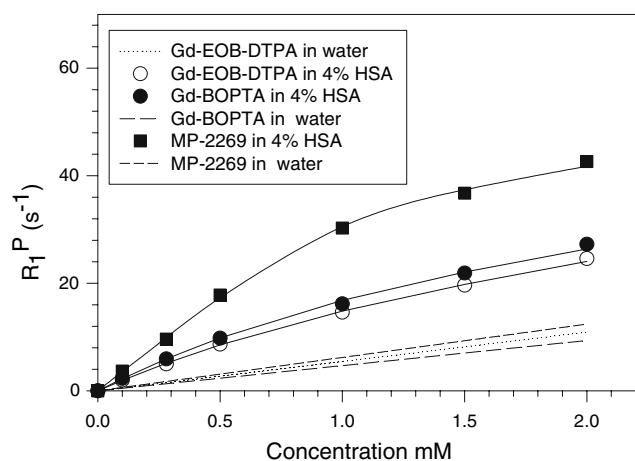


Fig. 4 Proton paramagnetic relaxation rate of aqueous 4% human serum albumin (HSA) solution containing increasing amounts of contrast agent; the *continuous lines* correspond to the fitting of the data and the *dashed lines* represent R_1^p in a water solution free of albumin (experimental data points not shown)

association constant (K) characterizing the interaction between HSA and the contrast agents and a value of the relaxivity of the covalently bound complex (r_1^c). Table 2 collects results obtained for Gd-EOB-DTPA, Gd-BOPTA, MP-2269, and published data on MS-325 [25]. Gd-EOB-DTPA and Gd-BOPTA behave quite similarly in the presence of HSA and have a moderate and similar affinity for the protein. MP-2269 binds more strongly to the protein with a stoichiometry close to 2. MS-325 shows a lower affinity for HSA than MP-2269. Unfortunately, proton relaxometry experiments with B-22956/1 could not be performed. However, at 20 MHz and the same concentration, MP-2269 and B-22956/1 have, respectively, an apparent relaxivity of 18 and 27 $\text{s}^{-1} \text{mM}^{-1}$ in HSA, indicating a stronger affinity of B-22956/1 for HSA than MP-2269. It is to be noticed that the model used to fit the relaxometry data involves several important limitations. First, all sites are assumed to be identical and independent. This is surely inaccurate for some contrast agents. Second, the relaxivity in the bound state is assumed to be identical in the different binding sites. This is a rough approximation since local

Table 2 Results of the fittings of the relaxometry data according to Eq. 1

	K (10^3 M^{-1})	N	r_1^c ($\text{s}^{-1} \text{mM}^{-1}$)	r_1^f ($\text{s}^{-1} \text{mM}^{-1}$)
Gd-EOB-DTPA	1.5 ± 0.5	0.9 ± 0.3	37.3 ± 16.8	6.0 ± 1.0
Gd-BOPTA	1.5 ± 0.5	1.0 ± 0.4	42.9 ± 11.1	5.2 ± 0.7
MP-2269	16.0 ± 6.9	1.6 ± 0.1	38.0 ± 7.4	6.5 ± 0.3
MS-325 ^a	6.8 ± 0.6	1.00 ± 0.06	48.0 ± 6.7	5.6 ± 0.1

^a From [25]

mobility, water exchange, and accessibility can be different in each binding site.

Electrospray mass spectrometry method

HSA has a molecular mass of about 66,437 Da [26]. Some publications on the application of ESI-MS to biological compounds showed spectra of HSA and bovine serum albumin recorded in positive ion mode [27–31]. All these spectra are very complex, owing to the presence of numerous peaks corresponding to the protein in different charge states. The minimum number of charges is about 40 positive charges. As mentioned by the authors, the very high number of charge states is a possible indication of partial denaturation.

In order to use mass spectrometry as a complementary or standalone technique to study the affinity between contrast agents and HSA, it is important to use conditions that keep the protein in its native state and that limit the formation of adducts with the macromolecule. In a previous report [32], we showed that an ammonium acetate solution was preferable to a solution of acetonitrile–water (Fig. 5). The peaks at a low mass-to-charge ratio are likely to be due to an unfolded state of the protein.

It is assumed that the lower accessibility of basic residues in the folded structure makes them less available for ionization than in the unfolded state. However, a direct relationship between the total number of basic amino acid residues and the maximum number of positive charges observed is not obvious since changes in the protein environment, such as pH or solvent conditions, may cause denaturation of the protein [33–35].

Gd-EOB-DTPA and Gd-BOPTA

In a previous work no significant change was noticed in the spectrum of HSA at an equal concentration of protein and ligand (Gd-EOB-DTPA). It was necessary to increase the concentration of Gd-EOB-DTPA to 20 μM in order to observe a peak corresponding to a 1:1 complex of HSA and Gd-EOB-DTPA [32]. Similar results were obtained here with Gd-BOPTA (Fig. 6).

MP-2269, MS-325, and B-22956/1

At identical concentrations of HSA and contrast agent (5 μM), four charge states of HSA alone (from 15+ to 18+) with additional peaks corresponding to a complex between HSA and one ligand were observed for MP-2269, MS-325, and B-22956/1. At this concentration, B-22956/1 showed the strongest interaction (Fig. 7). When the concentration of ligand was twice the concentration of protein (Fig. 8), the signals corresponding to the 1:1 complex with MS-325

Fig. 5 Mass spectra of HSA dissolved in ammonium acetate buffer (a) and in acetonitrile buffer (b)

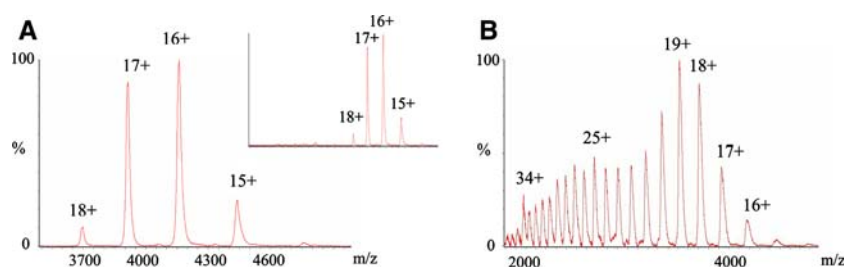


Fig. 6 Mass spectra of HSA (5 μ M) with 20 μ M Gd-EOB-DTPA (a) and 20 μ M Gd-BOPTA (b)

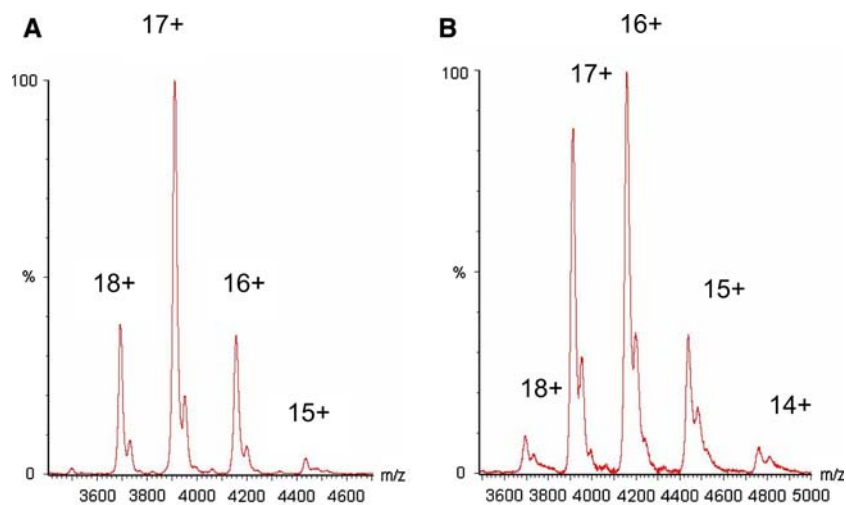


Fig. 7 Mass spectra of HSA (5 μ M) with 5 μ M MP-2269 (a), 5 μ M MS-325 (b), and 5 μ M B22956/1 (c)

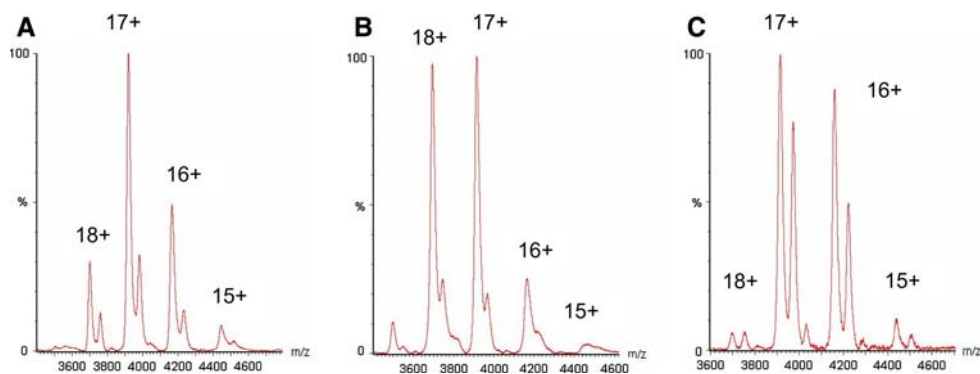
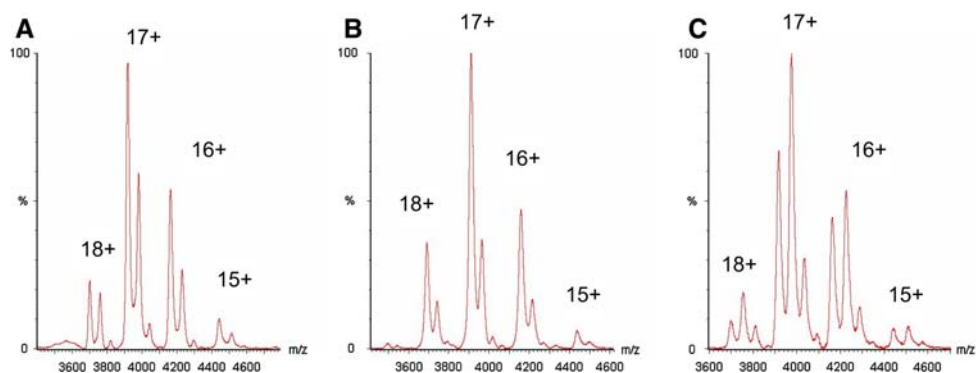
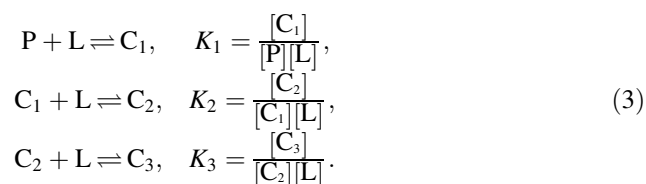


Fig. 8 Mass spectra of HSA (5 μ M) with 10 μ M MP-2269 (a), 10 μ M MS-325 (b), and 10 μ M B22956/1 (c)



were more intense. For MP-2269, a second signal was observed corresponding to a stoichiometry 1:2. For B-22956/1, an additional complex (1:2) was also observed and the intensity of the peaks corresponding to the free protein decreased, indicating a very strong affinity. At a concentration of contrast agents of 20 μM (Fig. 9), MS-325 showed three complexes (1:1, 1:2, 1:3), whereas the stoichiometry for MP-2269 (1:1 and 1:2) was preserved and the peaks of the free protein decreased. In these same conditions, a new stoichiometry (1:3) appeared for B-22956/1 and a concomitant decrease of the peaks corresponding to the protein alone was observed. For a tenfold molar excess (Fig. 10), a decrease of the peaks corresponding to HSA alone with a stoichiometry of 3 was observed for MS-325. For MP-2269, a new stoichiometry appeared (1:3), while the stoichiometry was unchanged for B-22956/1.

These titration experiments provided qualitative information about the affinity of the contrast agents for HSA: B-22956/1 has a very strong affinity for the protein, MS-325 and MP-2269 seem to have a strong affinity, while Gd-EOB-DTPA and Gd-BOPTA show a weaker affinity. In order to get quantitative information on the binding, the electrospray mass spectrometry spectra were mathematically treated using the program MaxEnt1TM. The peak area of the various multiply charged ions of the free protein and of the protein–contrast agent complexes were added to evaluate their respective concentrations. The program uses the maximum-entropy method to reconstruct neutral molecular mass spectra from spectra of multiply charged forms [32]. Thanks to this treatment, the concentrations of the different species were obtained and allowed for the calculation of the different affinity constants named K_1 , K_2 , and K_3 (Eq. 3):



For each contrast agent, K_1 , K_2 , and K_3 were calculated for the samples containing 5 μM HSA and 20 μM contrast agent (Table 3).

The strongest interaction is observed with B-22956/1, with an affinity constant of about 260,000 M^{-1} for the first site. MP-2269 and MS-325 have lower and similar affinities (about 50,000 M^{-1}). Gd-EOB-DTPA and Gd-BOPTA show weak and similar affinities (about 5,000 M^{-1}). One of the greatest benefits of electrospray ionization for the study of non-covalent interactions is the knowledge of the stoichiometry. This information is obtained directly from the spectrum. Since the electrospray mass spectrometry showed a stoichiometry of 2 for MP-2269, the number of high-affinity sites was set to 2 in a new fit of the ultrafiltration data. The parameters obtained after this new treatment are as follows: $n_1 = 2$, $K_1 = (14.3 \pm 3.5) \times 10^3 \text{ M}^{-1}$, $n_2 = 17 \pm 24$, $K_2 = (0.15 \pm 0.25) \times 10^3 \text{ M}^{-1}$.

Conclusions

The study of the affinity of contrast agents for HSA, carried out by proton relaxometry, ultrafiltration, and electrospray mass spectrometry, showed a parallel trend (Table 4).

The weaker values of the association constants obtained by ultrafiltration for Gd-EOB-DTPA and Gd-BOPTA are probably due to the presence of salt (150 mM NaCl), which was added to the solution to minimize the Donnan effect. Association constants obtained by electrospray mass spectrometry follow the same trend as those estimated by the other techniques but with higher values, since the electrostatic forces are increased in the gas phase. Electrospray mass spectrometry is a fast method requiring the smallest quantity of product. The amount of contrast agent and the amount of protein needed are in the nanomolar range, while ultrafiltration and relaxometry need a few micromoles. More important, mass spectrometry gives direct information on the stoichiometry. With the majority of the alternative techniques, this information appears as a

Fig. 9 Mass spectra of HSA (5 μM) with 20 μM MP-2269 (a), 20 μM MS-325 (b), and 20 μM B22956/1 (c)

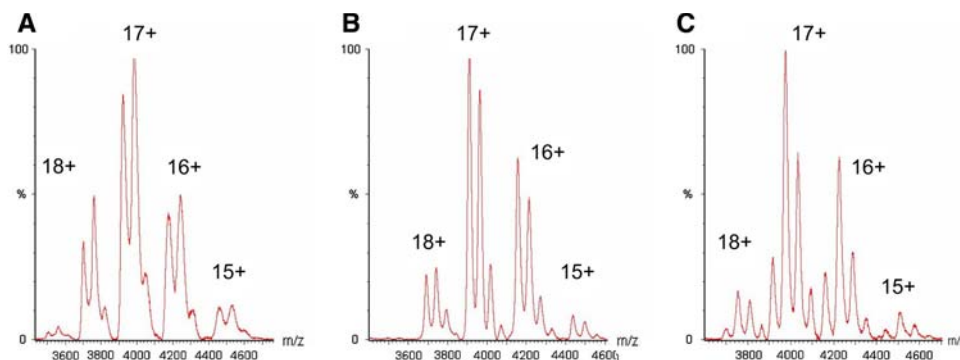


Fig. 10 Mass spectra of HSA (5 μ M) with 50 μ M MP-2269 (a), 50 μ M MS-325 (b), and 50 μ M B22956/1 (c)

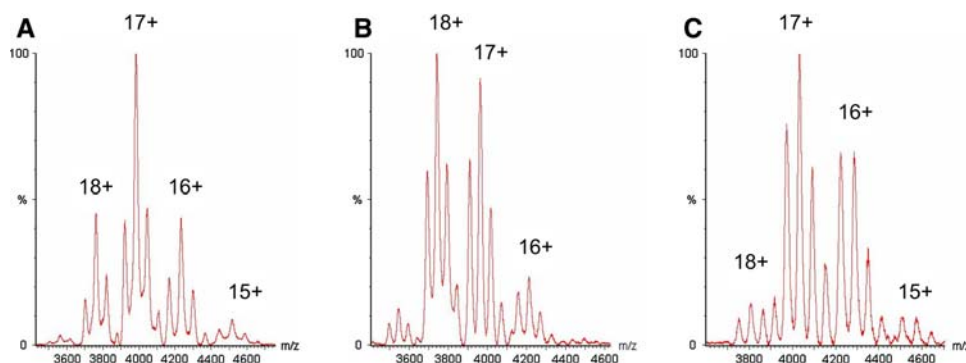


Table 3 The electrospray ionization association constants calculated from spectra treated by MaxEnt1TM according to Eq. 3

	K_1 (10^3 M ⁻¹)	K_2 (10^3 M ⁻¹)	K_3 (10^3 M ⁻¹)
Gd-EOB-DTPA	5.3	–	–
Gd-BOPTA	5.6	–	–
MP-2269	50	19	–
MS-325	46	19	–
B-22956/1	261	39	20

Table 4 Comparison of the association constants obtained by ultrafiltration, proton relaxometry, and mass spectrometry

	K ultrafiltration (10^3 M ⁻¹)	K proton relaxometry (10^3 M ⁻¹)	K mass spectrometry (10^3 M ⁻¹)
Gd-EOB-DTPA	0.3 ($n = 1$)	1.5 ($n = 1$)	5.3 ($n = 1$)
Gd-BOPTA	0.2 ($n = 1$)	1.5 ($n = 1$)	5.6 ($n = 1$)
MS-325	11 ($n = 1$) ^a	6.8 ($n = 1$) ^b	46 ($n = 1$)
MP-2269	14 ($n = 2$)	16 ($n = 2$)	50 ($n = 1$)
B-22956	260 ($n = 1$) ^c	–	261 ($n = 1$)

^a From [16]

^b From [25]

^c From [23, 24]

parameter obtained from the fitting. Ultrafiltration remains an important classic method for the determination of the affinity. It allows one to work in physiological conditions (4% HSA) and to obtain the affinity of strong and weak sites. Unlike the previous two methods, proton relaxometry is restricted to the study of paramagnetic systems. It is, however, essential to evaluate the efficiency of an MRI contrast agent since good affinity is not necessarily the sign of good efficiency. Indeed, the presence of a water molecule close to the paramagnetic ion and its fast exchange with the bulk as well as the mobility of the complex determine its efficiency as an MRI contrast agent. For example, a contrast agent strongly bound to a macromol-

ecule but having no water molecule in its first coordination sphere will not be a good MRI contrast agent [36].

Acknowledgements The support and sponsorship provided by COST Action D18 ‘‘Lanthanide Chemistry for Diagnosis and Therapy’’, the ARC Program of the French Community of Belgium, the FNRS and the EMIL NoE of the FP6 are also gratefully acknowledged. The authors thank Patricia de Francisco for her help in preparing the manuscript.

References

- Caravan P, Ellison JJ, McMurry TJ, Lauffer RB (1999) Chem Rev 99:2293–2352
- Toth E, Helm L, Merbach AE (2001) In: Merbach AE, Toth E (eds) The chemistry of contrast agents in medical magnetic resonance imaging. Wiley, London, pp 45–119
- Aime S, Botta M, Fasano M, Terreno E (2001) In: Merbach AE, Toth E (eds) The chemistry of contrast agents in medical magnetic resonance imaging. Wiley, London, pp 193–241
- Aime S, Gianolio E, Terreno E, Giovenzana GB, Pagliarin R, Sisti M, Palmisano G, Botta M, Lowe MP, Parker D (2000) J Biol Inorg Chem 5:488–497
- Aime S, Chiaussa M, Digilio G, Gianolio E, Terreno E (1999) J Biol Inorg Chem 4:766–774
- Parac-Vogt TN, Kimpe K, Laurent S, Vander Elst L, Burtea C, Chen F, Muller RN, Ni YC, Verbruggen A, Binnemans K (2005) Chem Eur J 11:3077–3086
- Aime S, Gianolio E, Longo D, Pagliarin R, Lovazzano C, Sisti M (2005) Chembiochem 6:818–820
- Vander Elst L, Maton F, Laurent S, Seghi F, Chapelle F, Muller RN (1997) Magn Reson Med 38:604–614
- Vander Elst L, Chapelle F, Laurent S, Muller RN (2001) J Biol Inorg Chem 6:196–200
- Cavagna FM, Marzola P, Dapra M, Maggioni F, Vicinanza E, Castelli PM, de Haen C, Luchinat C, Wendland MF, Saeed M, Higgins CB (1994) Invest Radiol 29:s50–s53
- Cavagna FM, Maggioni F, Castelli PM, Dapra M, Imperatori LG, Lorusso V, Jenkins BG (1997) Invest Radiol 32:780–796
- Wallace RA, Haar JP, Miller DB, Woulfe SR, Polta JA, Galen KP, Hynes MR, Adzamlı K (1998) Magn Reson Med 40:733–739
- Adzamlı K, Spiller M, Koenig SH (2002) Acad Radiol 9:11–16
- Adzamlı K, Vander Elst L, Laurent S, Muller RN (2001) Magn Reson Mater Phys Biol Med 12:92–95
- Lauffer RB, Parmelee DJ, Dunham SU, Ouellet HS, Dolan RP, Witte S, McMurry TJ, Walovitch RC (1998) Radiology 207:529–538

16. Caravan P, Cloutier NJ, Greenfield MT, McDermid SA, Dunham SU, Bulte JWM, Amedio JC, Looby RJ Jr, Supkowski RM, Horrocks WDeW, McMurry TJ, Lauffer RB (2002) *J Am Chem Soc* 124:3152–3162
17. Zheng J, Carr J, Harris K, Saker MB, Cavagna FM, Maggioni F, Laub G, Li D, Finn JP (2001) *J Magn Reson Imaging* 14:425–432
18. Paetsch I, Huber ME, Bornstedt A, Schnackenburg B, Boesiger P, Stuber M, Fleck E, Cavagna F, Nagel E (2004) *J Magn Reson Imaging* 20:288–293
19. Wolfer GK, Barton Rippon W (1987) *Clin Chem* 33:115–117
20. Menguy T, Chenevois S, Guillain F, le Maire M, Falson P, Champeil P (1998) *Anal Biochem* 264:141–148
21. Loo JA (2000) *Int J Mass Spectrom* 200:175–186
22. Veenstra TD (1999) *Biophys Chem* 79:63–79
23. Cavagna FM, Lorusso V, Anelli PL, Maggioni F, de Haën C (2002) *Acad Radiol* 9:491–494
24. Cavagna FM, Lorusso V, Anelli PL, Maggioni F, de Haën C (2001) *CMR2001 Capri*, pp 42–44
25. Muller RN, Radúchel B, Laurent S, Platzek J, Piérart C, Mareski P, Vander Elst L (1999) *Eur J Inorg Chem* 1949–1955
26. Meloun B (1975) *FEBS Lett* 58–134
27. Chowdhury SK, Katta V, Chait BT (1990) *Rapid Commun Mass Spectrom* 4:81–87
28. Loo JA, Edmonds CG, Udseth HR, Smith RD (1990) *Anal Chem* 62:693–698
29. Smith RD, Loo JA, Edmonds CG, Barinaga J, Udseth HR (1990) *Anal Chem* 62:882–899
30. Bunk DM, Welch MJ (1997) *J Am Soc Mass Spectrom* 8:1247–1254
31. Baczynskyj L, Bronson GE, Kubiak TM (1994) *Rapid Commun Mass Spectrom* 8:280–286
32. Henrotte V, Laurent S, Gabelica V, Vander Elst L, Depauw E, Muller RN (2004) *Rapid Commun Mass Spectrom* 18:1919–1924
33. Lavarone AT, Jurchen JC, Williams ER (2000) *J Am Soc Mass Spectrom* 11:976–985
34. Grandori RJ (2003) *Mass Spectrom* 38:11–15
35. Grandori RJ (2003) *Curr Org Chem* 7:1589–1603
36. Laurent S, Vander Elst L, Muller RN (2006) *Contrast Med Mol Imaging* 1:128–137